Proceedings of the 20th International Conference on Soil Mechanics and Geotechnical Engineering– Rahman and Jaksa (Eds)

Investigating the shear strength uniqueness and failure state behaviour of loess-waste straw mixture considering stress path effect

Enquête sur l'unicité de la résistance au cisaillement et du comportement de l'état de défaillance du mélange de lœss et de déchets de paille en prenant en compte de l'effet du chemin de stress

Wen-Chieh Cheng, Lin Wang & Zhong-Fei Xue
School of Civil Engineering, Xi'an University of Architecture and Technology, Shaanxi Key Laboratory of Geotechnical and Underground Space Engineering (XAUAT), China, w-c.cheng@xauat.edu.cn

ABSTRACT: A significant body of research conducted over the past decades indicate that the macroscale material mechanical behaviour relies upon not only the stress state but also the loading regime. The loess-waste straw mixture, which is easily accessible in the Chinese Loess Plateau and widely applied to the construction of rural houses that have been inhabited for decades under the effect of freeze-thaw cycles, was used to prepare cylinder specimens. A higher degree of saturation for the specimens was achieved with a combination of vacuum saturation and back pressure saturation. The specimens consolidated along the isotropic compression path at consolidating pressures varying in 200-400 kPa to backtrack their initial stress states. In stress-path tests, various stress paths, namely conventional triaxial compression (CTC), reduced triaxial compression (RTC), conventional triaxial extension (CTE), and reduced triaxial extension (RTE) were considered, and strain rate and loading rate control measures were to minimise the impacts of strain (or loading) on the strength characteristics of the unreinforced and reinforced loess. The test results highlighted the role of straw fiber inclusion and orientation in the increase of shear strength and the importance of the effect of stress path on the shear strength uniqueness and the failure state behaviour.

RÉSUMÉ : Selon un important corpus de recherches effectuées au cours des dernières décennies, le comportement mécanique macroscopique des matériaux dépend non seulement de l'état de stress, mais aussi du régime de charge. Le mélange de lœss et de déchets de paille, facilement accessible dans le plateau de lœss chinois et largement appliqué à la construction de logements ruraux habités depuis des décennies sous l'effet des cycles de gel-dégel, a été utilisé dans la préparation des échantillons de cylindre. À travers la combinaison de saturation sous vide et de saturation de contre-pression, on a obtenu un degré de saturation plus hauts pour les échantillons Les échantillons se sont consolidés le long du chemin de compression isotrope à des pressions de consolidation variant de 200 à 400 kPa afin de revenir sur leurs états de stress initiaux. Dans les tests de chemin de stress, on a pris en compte divers chemins de tress, y compris la compression triaxiale conventionnelle (CTC), la compression triaxiale réduite (RTC), l'extension triaxiale conventionnelle (CTE) et l'extension triaxiale réduite (RTE), et pris des mesures de contrôle du taux de contrainte et du taux de charge dans le but de minimiser les impacts de la déformation (ou de la charge) sur les caractéristiques de résistance du lœss renforcé et non renforcé. Les résultats des tests ont souligné le rôle de l'inclusion et de l'orientation des fibres de paille dans l'amélioration de la résistance au cisaillement et l'importance de l'effet du chemin de stress sur l'unicité de la résistance au cisaillement et le comportement de l'état de défaillance.

KEYWORDS: stress path, triaxial test, waste straw, shear strength, failure state behaviour.

1 INTRODUCTION

The Loess Plateau confronts serious water and soil preservation issue due to the overdevelopment of land, which has caused an eco-environmental crisis and also affected the livelihood of local farmers in China (Qiu et al. 2017). It is widely recognized that various scales of catastrophic slope sliding and instability have been caused by erosion-prone loess (Wu et al 2018; Zhang et al. 2010). At present, a significant body of research has recognized that fibers are deemed effective in preventing and controlling soil erosion. Further, many studies on fiber-reinforced soils also indicated that the macroscale material mechanical behaviour of fiber-reinforced soils relates not only to stress state but also to loading regime (e.g. Ng et al. 2003; Finno & Kim 2012; Liu et al. 2019; Wang et al. 2020). Thus, there is a pressing need to study the fiber-reinforced soil to reveal its mechanical behaviour when subjected to different external loads (e.g. Hoyos et al. 2010; Jiang et al. 2017).

Recent researches including laboratory studies and post-event analysis have attempted to explore the potential for the use of the waste straw fiber. The use of straw fiber to reinforce the loess assessed using direct shear tests towards determining the optimal fiber dosage and proposing the formation mechanism of enhanced shear strength (Cheng et al. 2019). Lian et al. (2019) studied the shear strength of the loess reinforced with plant root through consolidated-undrained triaxial tests considering the effect of root distribution and moisture content. Qu et al. (2016) also evaluated the consolidation characters and shear strength behaviour of the reinforced Shanghai clayey soil. The results showed that there is an optimum addition content with a significant increase in shear strength and friction angle under one-dimensional consolidation and triaxial tests. To sum up, the use of agricultural waste seems to impose a positive effect on the shear strength of the soils because of its superior load transfer and distribution ability. Nevertheless, studies exploring the stress-strain relation and the pore pressure behaviour of the reinforced loess subjected to different stress paths and fiber dosages and comparing them to the unreinforced loess are remarkably limited.

The aims of this study are: (a) to characterise the stress-strain relation and the pore pressure behaviour of the unreinforced and reinforced loess subjected to different stress paths, (b) to highlight the effect of straw fiber inclusion on the increase in

shear strength, (c) to evaluate the failure state behaviour uniqueness in p'-q space and e-logp' space respectively towards providing some guideposts in erosion prevention and mitigation.

2 EXPERIMENTAL STUDY

2.1 *Specimen preparation*

The Lantian loess has a specific gravity G_s of 2.69 and consists of 92.12% fines and 7.88% sand. The liquid limit LL is 31.6, while the plastic limit PL is 19.5. The Lantian loess is, therefore, classed as low-plasticity clay (CL), in accordance with the Unified Soil Classification System (USCS). The physical properties of the loess are summarized in Table 1.

In this work, a series of remolded cylinder specimens of 80 mm in height and 39.1 mm in diameter were trimmed to conduct the stress-path controlled triaxial shearing tests. The dimensions of the straw fiber included in the cylinder specimens are about 10 mm in length, and 4 mm in width. The straw fibers were first treated using boiling water for the sake of cylinder specimen preparation. The dosage of 0.6% addition was considered, according to the work of Cheng et al. (2019).

Table.1 Physical properties of tested loess.

LL (%)	PL (%)	G_s	Fines (%)	Sand (%)	γ_d (g/cm^3)	USCS symbol
31.6	19.5	2.69	92.1	7.9	1.4	CL

2.2 *Stress-path testing*

The unreinforced and reinforced loess specimens were isotropical consolidated and sheared in an undrained manner using conventional triaxial compression (CTC), reduced triaxial compression (RTC), conventional triaxial extension (CTE), and reduced triaxial extension (RTE) stress paths. A rather slow rate of 0.05%/min for the specimens shears under CTC and RTE paths was introduced, while for those sheared under RTC and CTE stress paths a very slow loading rate of 0.4kPa/min was minimising the impacts of strain (or loading) rate on the strength characteristics of soils and allowing pore pressure changes to be equalized throughout the remolded specimens (Deli & Vasarhelyi 2000; Artkhonghan et al. 2018; Ignat et al. 2019).

3 RESULTS

3.1 *Conventional triaxial compression*

3.1.1 *Undrained stress-strain behaviour*

The consolidated undrained stress-strain relation of unreinforced loess and reinforced loess confined at pressures σ_3 of 200, 300, and 400 kPa under the CTC stress path is shown in Figure 1. The deviatoric stress q was found to increase with an increase in confining pressure, with a higher rate of increase observed for the reinforced loess. In the case of reinforced loess, q increased sharply at lower strains of up to 4%, and, thereafter, gradually as strain values moved towards 20%.

3.1.2 *Pore pressure behaviour*

The pore pressure response of unreinforced loess and reinforced loess is presented in Figure 2. The pore pressure u for the unreinforced loess increased very quickly at lower strains for all confining pressures, and after reaching a peak value, a subtle fall in pore pressure was observed at higher strains. However, the reinforced loess showed a continuous increase in u for all the confining pressures.

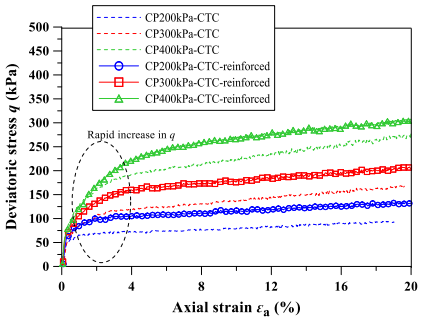

Figure 1. Undrained stress-strain relation of unreinforced loess and reinforced loess under the CTC stress path.

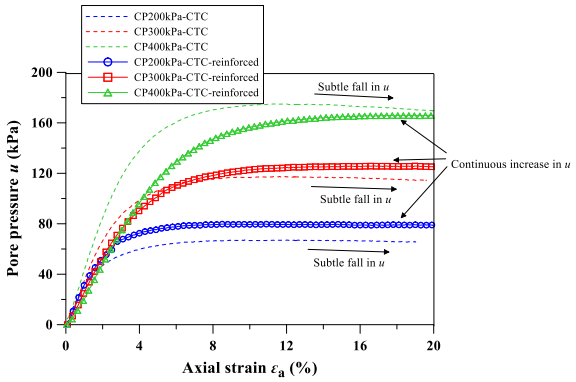

Figure 2. Pore pressure response of unreinforced loess and reinforced loess under the CTC stress path.

3.2 *Reduced triaxial compression*

3.2.1 *Undrained stress-strain behaviour*

The consolidated undrained stress-strain relation of unreinforced loess and reinforced loess under the RTC stress path for three confining pressures is shown in Figure 3. q was found to increase with the increase of σ_3, with a higher rate of increase observed for the reinforced loess. The higher the confining pressure, the higher the rate of increase in q. q went up very rapidly at lower strain values of up to 2%, and after moved towards 20%.

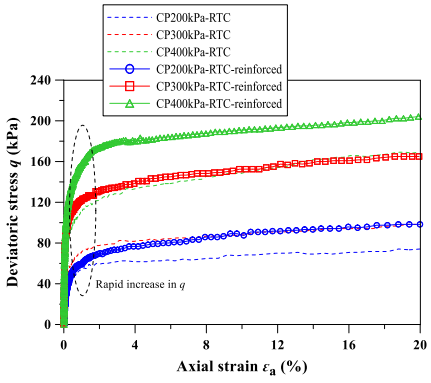

Figure 3. Undrained stress-strain relation of unreinforced loess and reinforced loess under the RTC stress path.

3.2.2 *Pore pressure behaviour*

The pore pressure response of unreinforced loess and reinforced loess is shown in Figure 4. u decreased initially at lower strains for all confining pressures, and after reaching a curve turning point, a rapid increase in u was observed at strains of 1-8%. Then u remained approximately unchanged at higher strain values for the reinforced loess and went into a decline for the unreinforced loess.

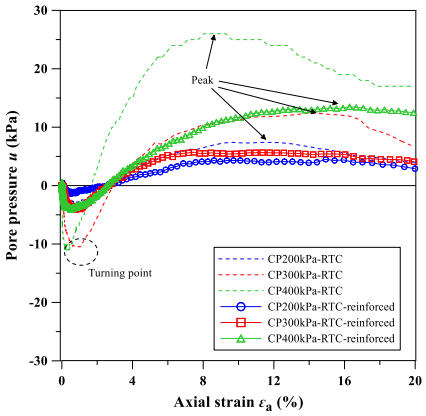

Figure 4. Pore pressure response of unreinforced loess and reinforced loess under the RTC stress path.

3.3 *Reduced triaxial extension*

3.3.1 *Undrained stress-strain behaviour*

The consolidated undrained stress-strain relation of unreinforced loess and reinforced loess under RTE stress path for three confining pressures is shown in Figure 5. q went up very quickly at lower strain values of up to 2%, and after reaching peak stress, a fall in q was observed at strains of 4-8%. The peak q values for the unreinforced loess were greater than that for the reinforced loess. The higher the confining pressure, the higher the q value.

3.3.2 *Pore pressure behaviour*

The pore pressure response of unreinforced loess and reinforced loess is shown in Figure 6. u increased initially at lower strains for all confining pressures, and at strains of 6-14%, u went into a decline. u increased again after 14% strain. Further, u for the reinforced loess was greater than that for the unreinforced loess.

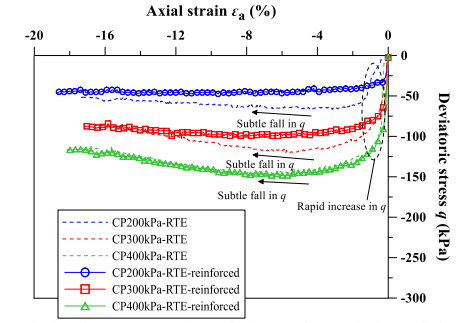

Figure 5. Undrained stress-strain relation of unreinforced loess and reinforced loess under the RTE stress path.

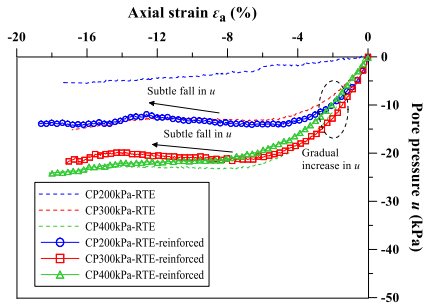

Figure 6. Pore pressure response of unreinforced loess and reinforced loess under the RTE stress path.

3.4 *Conventional triaxial extension*

3.4.1 *Undrained stress-strain behaviour*

The undrained stress-strain relation of unreinforced loess and reinforced loess under the CTE stress path for three confining pressures is shown in Figure 7. q was observed to increase with the increase of σ_3. Further, the higher the σ_3 value, the higher the q value. q for the reinforced loess was greater than that for the unreinforced loess.

3.4.2 *Pore pressure behaviour*

The pore pressure response of unreinforced loess and reinforced loess is shown in Figure 8. It is evident that u showed a rapid increase at small strain ranges and no longer increased at strains beyond 4%. u for the reinforced loess was smaller than that for the unreinforced loess confined at all confining pressures.

4 DISCUSSION

4.1 *Stress-strain relation and stress path character*

It is evident that the stress-strain relation of the unreinforced loess and the reinforced loess under the CTC stress path, RTC stress path, and CTE stress path is featured with strain-hardening behaviour (Figures 1, 3, and 7). In contrast, the stress path of the unreinforced loess and the reinforced loess under the RTE stress path exhibits a strain-softening behaviour (Figure 5).

The effective stress paths of the unreinforced loess and the reinforced loess sheared under the four stress paths respectively are shown in Figure 9. The strain-hardening behaviour of the unreinforced loess and the reinforced loess under the CTC stress path was accompanied by the increase of the mean stress p' and then the decrease of the mean stress p' towards specimen failure. It is noteworthy that the effective stress paths were not ended when failed and in turn, traveled a certain distance along the failure line (FL). Such effective stress paths suggest that the unreinforced loess and the reinforced loess was contractive in the first place, followed by a phase transformation and then dilative behaviour. The strain-hardening behaviour of the unreinforced loess and the reinforced loess under the RTC stress path was accompanied by the decrease of p' towards failure. Unlike the CTC stress path, the effective stress paths stopped when failed and no further movement was observed, meaning that the unreinforced loess and the reinforced loess was dilative throughout. During the extension tests, the failure of specimen is mostly characterised by a localised deformation present at its middle part, referred also to as the 'necking' phenomenon. The necking phenomenon of the unreinforced loess and the reinforced loess under the CTE stress path occurred right before the increase of p' where the slope in the u-ε_a plot became negative. Further, the unreinforced loess and the reinforced loess was contractive throughout. On the other hand, the necking behaviour of the unreinforced loess and the reinforced loess under the RTE stress path occurred with the decrease of p'. The unreinforced and reinforced loess was contractive all long.

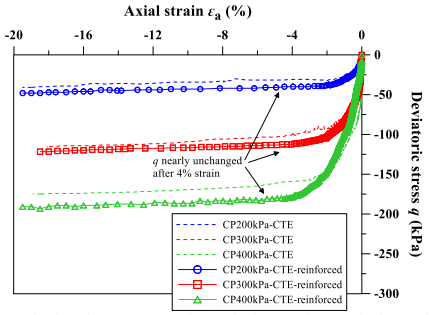

Figure 7. Undrained stress-strain relation of unreinforced loess and reinforced loess under the CTE stress path.

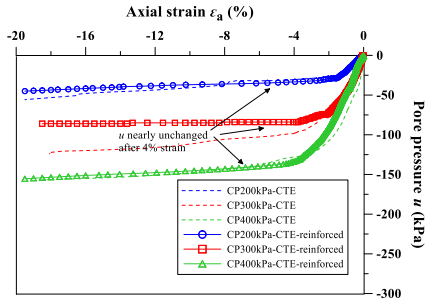

Figure 8. Pore pressure response of unreinforced loess and reinforced loess under the CTE stress path.

4.2 *Comparison between unreinforced loess and reinforced loess and formation mechanism of enhanced shear strength*

u of the reinforced loess confined at σ_3 = 200 kPa and 300 kPa respectively under the CTC stress path was higher than that of the unreinforced loess when subjected to the undrained shearing. The straw fiber inclusion caused some difficulty in developing the relative displacement between straw fibers and soil particles in the shear band towards causing the higher u for the reinforced loess (Li 2005). In light of this, the reinforced loess could provide a superior shear strength against large shear stresses. u for the reinforced loess for the same confining pressure under the RTC stress path was lower than that for the unreinforced loess.

The shear strength of the reinforced loess under extension can be improved by transferring the tension along the length of straw fibers oriented in a vertical direction. Thus, the straw fibers oriented other than the vertical direction may not contribute to the increase in shear strength. Further, the orientation of the straw fibers depends not only upon specimen preparation but also upon the gravity effect. On the other hand, Peters and Berney (2010) indicated that the stress-strain relation can notably be influenced by the fiber inclusion and that the strength of the soil increases with increasing the fiber content up to an optimum fiber dosage. It can be seen that q for the reinforced loess under the RTE stress path was lower than that for the unreinforced loess. In contrast, q for the reinforced loess under the CTE stress path was higher than that for the unreinforced loess. The development of the shear plane along the straw fiber-soil particle interface was deemed to be the main cause leading to this phenomenon. Furthermore, σ_3 remained constant throughout the RTE stress path brought benefit to the development of the shear plane.

4.3 *Strength envelopes*

The strength envelopes derived from the stress-path tests are shown in Figure 10. ϕ' derived from the strength envelopes resulting from the CTC tests is 23.6° for the unreinforced loess and 26.6° for the reinforced loess. ϕ' derived from the envelopes resulting from the RTC tests is 18.4° for the unreinforced loess and 21.8° for the reinforced loess. Under the RTE stress path, ϕ' is 16.3° for the unreinforced loess and 21° for the reinforced loess. Under the CTE stress path, ϕ' for the unreinforced loess is 22.7° which is slightly smaller than 23° for the reinforced loess. On the whole, the shear strengths of the loess under the compression tests were greater than those of the loess under the extension tests. The constraint on the relative displacement within the shear band between the straw fiber and soil particle was considered to be the main contributor to the enhanced shear strength. Further, the reinforced loess, featured with a better ability against large shear deformation than the unreinforced loess, under the extension tests was because of the distribution of shear stresses along the length of straw fibers. This especially holds true when subjected to the straw fiber oriented in the vertical direction. Amongst the four stress paths, the shear strengths for the loess under the CTC stress path were the highest, and the shear strengths for the loess under the RTE stress path were the lowest. These results confirmed the un-identifiability of a unique FL under different stress paths.

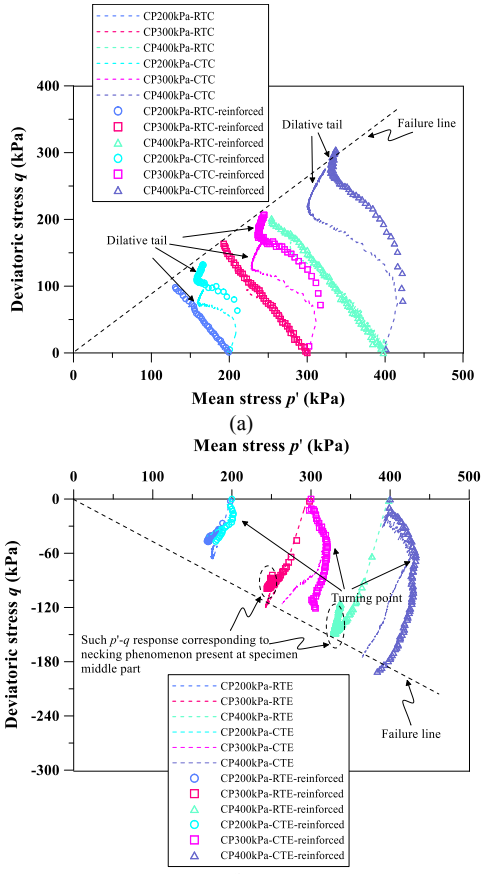

Figure 9. Effective stress paths of unreinforced loess and reinforced loess in p'- q space: (a) CTC and RTC stress paths; (b) RTE and CTE stress paths.

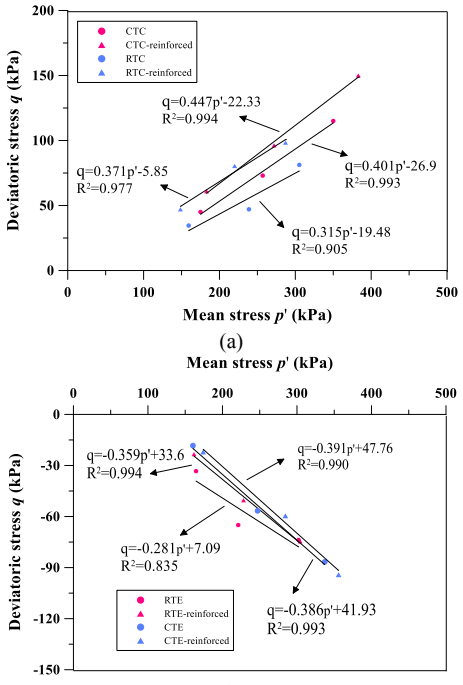

Figure 10. Strength envelopes of unreinforced loess and reinforced loess in p'- q space: (a) CTC and RTC stress paths; (b) RTE and CTE stress paths.

4.4 *Failure state behaviour*

Failure state behaviour was analysed and used to provide a better explanation regarding the effect of fiber reinforcement inclusion on the enhancement of the mechanical properties. q' was first normalised using σ_3 towards eliminating the effect of confining pressure. The relationships of normalised q' versus axial strain ε_a for the unreinforced and reinforced loesses respectively under the compression and tension tests are shown in Figure 11. The normalised q' for the reinforced loess under the RTC stress path increased very rapidly at small ε_a range and reached the turning point when $\varepsilon_a = 2\%$ (see Figure 11a). The normalised q' showed a small change at large ε_a range. The relationship of normalised q' versus ε_a for the unreinforced loess under the same stress path developed in a similar manner compared to the reinforced loess. However, its normalised q' at large ε_a range was much lower than that for the reinforced loess. In contrast to the RTC stress path, when $\varepsilon_a = 5\%$ the normalised q' for the reinforced loess under the CTC stress path reached the turning point, which took place later than the RTC stress path (see Figure 12). Further, the normalised q' for the reinforced loess at large ε_a range was close to that for the unreinforced loess, which also indicated a lower significance of the effect of fiber inclusion. The more densified loess under the CTC stress path reduced the effect of fiber inclusion and caused the loess to contract first and to dilate after a phase transformation towards failure. On the other hand, the more loose loess highlighted the effect of fiber inclusion and differentiated the normalised q' versus ε_a relationship for the unreinforced and reinforced loess. Therefore, the loess dilated throughout towards failure.

The normalised q' for the loess under the CTE stress path increased rapidly at small ε_a range, and after reaching the turning point at ε_a = 4%, the normalised q' increased steadily towards failure (see Figures 11b and 12). In contrast to the CTE stress path, an increase in normalised q' at small ε_a range, followed by a decrease when ε_a in excess of 6%, was observed for the loess under the RTE stress path. Further, the loess under both the tension tests contracted all long towards failure. The normalised pore pressure versus ε_a relationship for the unreinforced and reinforced loesses respectively under the compression and tension tests are shown in Figure 13. The normalised pore pressure for the reinforced loess at σ_3 = 400 kPa, however, was lower than that for the unreinforced loess. These results were opposite to those resulting from σ_3 = 200 kPa and σ_3 = 300 kPa; the normalised pore pressure for the reinforced loess at σ_3 = 200 kPa and σ_3 = 300 kPa was higher than that for the unreinforced loess. The effect of fiber inclusion limited the relative movement between straw fiber and soil particles, hence developing the higher pore pressure and causing some difficulty in developing the shear plane. Despite that, the denser the specimen, the lower significance the effect of fiber reinforcement inclusion. This is to say, when σ_3 = 400 kPa the enhancement of the mechanical properties was not attributed to the friction against the straw fiber-soil particle interface but to the higher confining pressures. On the whole, the stress path primarily governed the failure state of the unreinforced and reinforced loess, although there was a difference of strain range for the loess to reach the yielding against different stress paths. The effect of fiber inclusion limited the relative movement between straw fibers and soil particles towards causing some difficulty in developing the shear plane and thus enhancing the mechanical properties of the loess. This enhancement, while performing the compression tests, was more significant when subjected to lower confining pressures. The higher pore pressures further justified the observed phenomenon. Further, the effect of fiber inclusion was more significant for the compression tests than that for the tension tests.

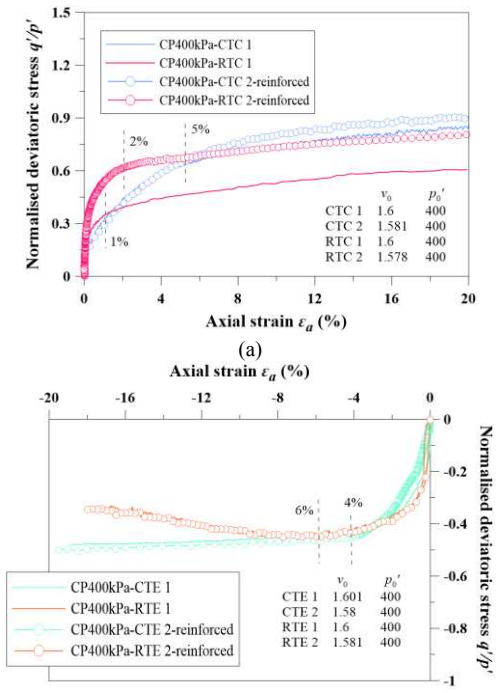

Figure 11. Normalised deviatoric stress versus axial strain relationship: (a) CTC and RTC stress paths (b) RTE and CTE stress paths.

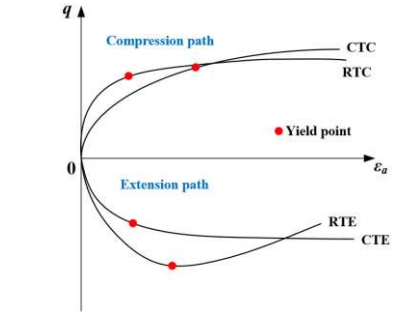

Figure 12 Occurrence of the yield point against different stress paths

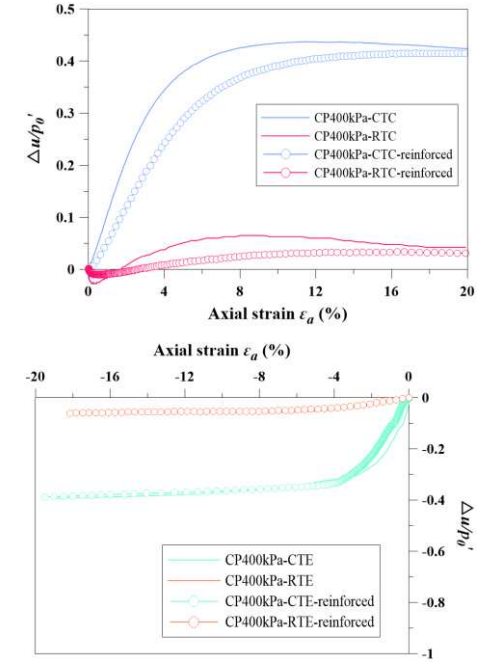

Figure 13. Normalised pore pressure versus axial strain relationship: (a) CTC and RTC stress paths (b) RTE and CTE stress paths.

5 CONCLUSIONS

The unreinforced and reinforced loesses were both sheared under four stress paths. The formation mechanism of the enhanced shear strength for the reinforced loess sheared under different stress paths was revealed. Based on the results and discussion, some main conclusions can be drawn as follows:

(1) The effective stress paths show that the loess under the CTC stress path was contractive firstly, followed by a phase transformation and then dilative behaviour. The loess under the RTC stress path was dilative throughout, and no phase transformation was observed. p' of the loess under RTE stress path was observed to decrease firstly and then increased with an increase of q. p' of the loess under the CTE stress path increased first and then decreased towards failure. The necking at both the specimens' middle part presented right after the increase of p'.

(2) Amongst the four stress paths, the shear strength of the loess under the CTC stress path was the highest, and the shear strength of the loess under the RTE stress path was the lowest. The shear strength for the compression tests was higher than that for the extension tests. The effect of fiber inclusion caused some difficulty for the loess under the CTC stress path to develop the relative movement between straw fibers and soil particles within the shear band. This was considered to be the main contributor to the highest shear strength. The higher u justified the observed phenomenon. Under the RTE stress path, the shear plane developed alongside with the straw fiber-soil particle interface, while the straw fiber oriented in the vertical direction still contributed to the increase of the shear strength. The necking at the specimen middle part, induced by the stress localisation, contributed to the reduced shear strength.

(3) The stress path dominated the failure state of the loess, while there was a difference of strain range for the loess to reach the yielding against different stress paths. The enhancement of the mechanical properties by the effect of fiber inclusion was more significant when subjected to lower confining pressures. The higher u of the unreinforced loess at σ_3 = 400 kPa provided a testimony of the observed phenomenon.

6 ACKNOWLEDGEMENTS

This work would not have been possible without supports from the Special Fund for Shaanxi innovation ability support scheme (EDS) under Grant no. 2020TD-005.

7 REFERENCES

Artkhonghan K., Sartkaew S., Thongprapha T. and Fuenkajorn K. 2018. Effects of stress path on shear strength of a rock salt. *International Journal of Rock Mechanics and Mining Sciences* 104, 78-83.

Cheng W.C., Xue Z.F., Lin W. and Xu J. 2019. Using post-harvest waste to improve shearing behaviour of loess and its validation by multiscale direct shear tests. *Applied Science* 9(23).

Deli A. and Vasarhelyi B. 2000. Investigation of the fracture process with different loading path triaxial tests on saturated sandstone. *Bulletin of Engineering Geology and The Enviroment* 59, 187-193.

Finno R.J. and Kim T. 2012. Effects of stress path rotation angle on small strain responses. *Journal of Geotechnical and Geoenvironmental Engineering* 138, 4.

Hoyos L.R., Perez R. Diego D. and Puppala A.J. 2012. Modeling unsaturated soil response under suction-controlled true triaxial stress paths. *International Journal of Geomechanics* 12(3), 292-308.

Ignat R., Baker S., Martin H. and Larsson S. 2019. Triaxial extension and tension tests on lime-cement-improved clay. *Soils and Foundations* 59(5), 1399-1416.

Jiang M.J., Sima J., Cui Y., Hu H., Zhou C. and Lei H. 2017. Experimental investigation of the deformation characteristics of natural loess under the stress paths in shield tunnel excavation. *International Journal of Geomechanics* 17(9).

Li C. 2005. Mechanical response of Fiber-Reinforced soil. Ph.D. Dissertation. The University of Texas at Austin, USA.

Lian B.Q., Peng J.B., Zhan H.B. and Wang X.G. 2019. Mechanical response of root-reinforced loess with various water contents. *Soil & Tillage Research* 193 (2019), 85–94.

Liu F.R., Zhou Z.W., Zhang S.J., Ma W. and Sun Z.Z. 2019. Experimental investigation of accumulation deformation properties of frozen silt clay under different cyclic stress-paths. *Cold Regions Ence and Technology* 163(2019), 108-118.

Ng C.W.W., Fung W.T., Cheuk C.Y. and Zhang L.M. 2003. Influence of stress ratio and stress path on behaviour of loose decomposed granite. *Journal of Geotechnical & Geoenvironmental Engineering* 130(1), 36-44.

Peters J.F. and Iv R.S.B. 2010. Percolation threshold of sand-clay binary mixtures. *Journal of Geotechnical & Geoenvironmental Engineering* 136(2), 310-318.

Qiu H., Cui P., Regmi A.D., Hu S., Wang X. and Zhang Y. 2017. Influence of topography and volume on mobility of loess slides within different slip surfaces. *Catena*. 157, 180-188.

Qu J. and Sun Z. 2016. Strength behaviour of shanghai clayey soil reinforced with wheat straw fibers. *Geotechnical & Geological Engineering*. 34(2), 515-527.

Wang L., Cheng W.C. and Xue Z.F. 2020. The Use of Agricultural Waste Straw to Enhance Loess Shearing Behaviour: An Experimental Investigation. *Advances in Materials Science and Engineering*. 2020, 12.

Wu L., Jiang J., Li G.X. and Ma X.Y. 2018. Characteristics of pulsed runoff-erosion events under typical rainstorms in a small watershed on the loess plateau of china. *Scientific Reports*. 8(1), 3672.

Zhang C.B., Chen L.H., Liu Y.P., Ji X.D. and Liu X.P. 2010. Triaxial compression test of soil-root composites to evaluate influence of roots on soil shear strength. *Ecological Engineering*. 36(1), 19-26.